Enhancing superconductivity with resonant antishielding and topological plasmon-polarons

Krzysztof Kempa [1,*] Nakib H. Protik [2] Tyler Dodge,[1] Claudia Draxl,[2] and Michael J. Naughton [1]

[1]*Department of Physics, Boston College, Chestnut Hill, Massachusetts 02467, USA*
[2]*Institut für Physik and IRIS Adlershof, Humboldt-Universität zu Berlin, 12489 Berlin, Germany*

By employing *ab initio* Migdal-Eliashberg calculations, we predict a fourfold enhancement of the superconducting critical temperature of MgB_2 when proximity-coupled to the topological crystal Bi_2Se_3. We support this result with calculations using the general Leavens scaling method. We show that this effect is a result of *dynamic resonant antishielding* of Cooper pairs by plasmon-polarons of Dirac electrons in the topological crystal. Our calculations show that such superconductivity enhancement varies strongly with Coulomb coupling between plasmon- polarons and Cooper pairs, with a pronounced maximum of T_c at a critical value of the coupling parameter. This feature is universal, and so can occur in other superconductor-topological crystal combinations, including with nonphonon mediated superconductors. We discuss methods to experimentally optimize the key coupling parameter.

I. INTRODUCTION

Increasing the critical temperature T_c of superconductivity toward room temperature has been a type of holy grail of physics. Discovery of the cuprate superconductors in the late 1980s, with T_c up to 92 K, rekindled the field, and raised hopes that room temperature could be in sight. Cuprate T_c was increased to 133 K [1] by 1993, but has since stalled there. Despite intense effort, similar sluggish progress has been made on the theoretical front, with the origin of cuprate superconductivity remaining insufficiently clear still today. Even though carrier bosonization remains a key concept, the pairing mechanism seems more subtle than the Bardeen-Cooper-Schrieffer (BCS) electron-phonon-electron interaction. In an early paper, Ginzburg and Kirzhnits [2] argued that there are no physical limits to prevent room temperature operation of BCS superconductors.

Separately, following an early reformulation of BCS theory in terms of an effective dielectric function [2,3,4], metallic metamaterials have been proposed to increase T_c by controlling the dielectric environment [5,6]. These can customize a dielectric response to obtain exotic optical properties [7], and were engineered to produce a small effective dielectric function, potentially capable of Cooper pair enhancement via antishielding. However, due to the locality of metamaterial dielectric response, only marginal T_c enhancements were observed [5,6]. Here, we demonstrate theoretically that dramatic T_c enhancements are possible via *resonant antishielding* (RAS), induced in the plasmon-polaron mode of the Dirac electrons on the surface of a topological crystal (TX) coupled to a superconductor, as sketched in Fig. 1.

II. RESONANT ANTISHIELDING

To illustrate the basic physics of antishielding, we begin with the standard model of a dressed electron-electron interaction in a jellium metal [8], containing the basics of the Migdal-Eliashberg theory:

$$\frac{V_q}{\varepsilon} + \left|\frac{g_q}{\varepsilon}\right|^2 \frac{2\omega_q}{(\omega^2 - \omega_q^2) + i\delta} = \frac{V_q}{\varepsilon_{\text{eff}}}, \quad (1)$$

where $V_q = 4\pi e^2/q^2$ is the bare electrostatic potential, ε the dielectric function of the environment, g_q the matrix element for electron-phonon scattering, averaged over all electronic states, ω_q the phonon dispersion, and $i\delta$ a small constant loss factor. The first term in is the screened electron-electron interaction, and the second, Fröhlich term is the electron-electron interaction mediated by phonons with frequency ω_q. Cooper pairing can occur at frequency $\omega \approx \omega_q$, with the wave vector q of the order of k_F (Fermi). Eq. (1) also shows that pairing can be strengthened by making $|\varepsilon| < 1$, i.e., antishielding, which represents enhancement, rather than suppression (shielding) of the interactions. RAS can occur if $|\varepsilon| \ll 1$. For a typical superconductor, $\varepsilon > 1$ and thus, antishielding is impossible without some additional mechanism. Similarly, conventional metamaterial structures cannot provide a RAS effect since, while vanishing of ε at $\omega \approx \omega_q$ is possible, achieving this at $q \sim k_F$ is exceedingly difficult, as this would require the smallest structured feature sizes to be of the order of $1/k_F$ [9]. Only surface roughness could provide such a minute corrugation. Also, the screening is much stronger for the Fröhlich term in Eq. (1); any more realistic treatment would require spectral averaging which, as a result of ε changing sign about the vanishing point, would lead to cancellations in the first term $\sim 1/\varepsilon$, and accumulations for the second, which goes as $1/|\varepsilon|^2$. The same holds for antishielding, including RAS.
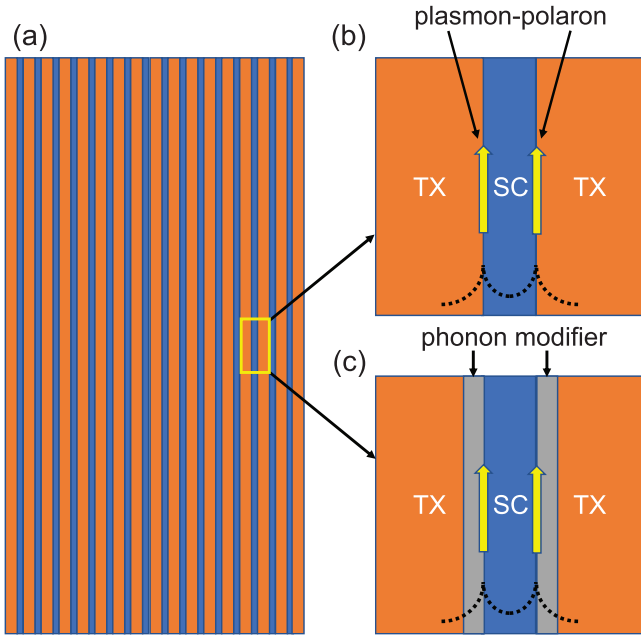
*Corresponding author: kempa@bc.edu

FIG. 1. (a) Superconductor (SC)-topological crystal (TX) superlattice structure designed to exploit the proposed resonant antishielding (RAS) effect produced by a surface plasmon-polaron. (b) Expanded view of the superlattice, also indicating the decaying amplitudes of the electric field (dashed lines) produced by the plasmon-polaron mode propagating (yellow arrows) along each interface. (c) Alternate structure containing additional phonon-modifier films. Note that, due to the topological proximity effect, plasmon-polaron modes occur at the interfaces of the modifiers with the superconductor.

Another strategy to achieve RAS lies in the fact that Maxwell's equations allow for the existence of longitudinal plasmon modes for which $\varepsilon(q, \omega) = 0$. However, conventional plasmon modes occur in a sector of phase space far from the required $\omega \approx \omega_q$ with q of the order of k_F. Recently, an unusual plasmonic α mode" was observed in the topo-

logical crystal Bi_2Se_3 [10], in that required phase space. The dispersion curve for this mode is close to linear, $\omega \propto q$ [Fig. 2(a)] and is clearly not a pure phonon mode, since it crosses the Brillouin zone (BZ) edge without any momentum Umklapp [10]. The most striking observation was that this mode remains strong and extremely weakly damped, with damping rate and intensity almost constant for $2k_F < q < 6k_F$ [11]. All other known plasmon modes are unobservable in that range. An interesting observation was that in the nontopological form of Bi_2Se_3, this α mode disappears and is replaced by a conventional, transverse acoustic phonon mode [Fig. 2(a)]. The new acoustic phonon mode has a standard dispersion, close to that of the α mode in the first BZ [10].

A recent theoretical study [11] is consistent with these discoveries. It shows that the α mode is a plasmon-polaron [12], a hybrid of plasmon excitations of Dirac surface electrons, and a transverse acoustic phonon mode. This α mode has topological character, with collective spin-charge fluctuations of the topological two-dimensional (2D) Dirac band states at the surface. Reference [11] demonstrated that the α mode has near perfect suppression of forward and backward scattering, resulting in ultralow damping, and an absence of Umklapp scattering at the BZ boundary. This α mode is similar to the phonon-polariton mode, a hybrid of photon and phonon excitations. To obtain the dispersion relation for the polariton [13], one starts with the dispersion relation for photons, $\omega = qc/\sqrt{\varepsilon}$, and replaces ε with the Lyddane-Sachs-Teller phonon formula [14], $\varepsilon = \varepsilon_{\text{eff}} = \frac{\omega_{LO}^2 - \omega^2}{\omega_{TO}^2 - \omega^2}$. By analogy, one can derive the dispersion for the plasmon-polaron by starting with the dispersion for the topological 2D Dirac plasmon [11], which contains $\overline{V_q} = V_q / \varepsilon$. We assume that $\varepsilon = \varepsilon_{\text{eff}}$, except now ε_{eff} is given by Eq. (1), with $\varepsilon = \bar{\varepsilon}$ (background dielectric constant). In the limit of interest in this work ($q \sim k_F$ and $\omega \sim \omega_q$), one gets

$$\varepsilon_{TI}(q, \omega) \approx 1 + \kappa |g_q|^2 \frac{2\omega_q}{(\omega^2 - \omega_q^2) + i\delta^2} \approx \frac{(\omega^2 - \bar{\omega}_q^2)}{(\omega^2 - \omega_q^2) + i\delta^2}$$
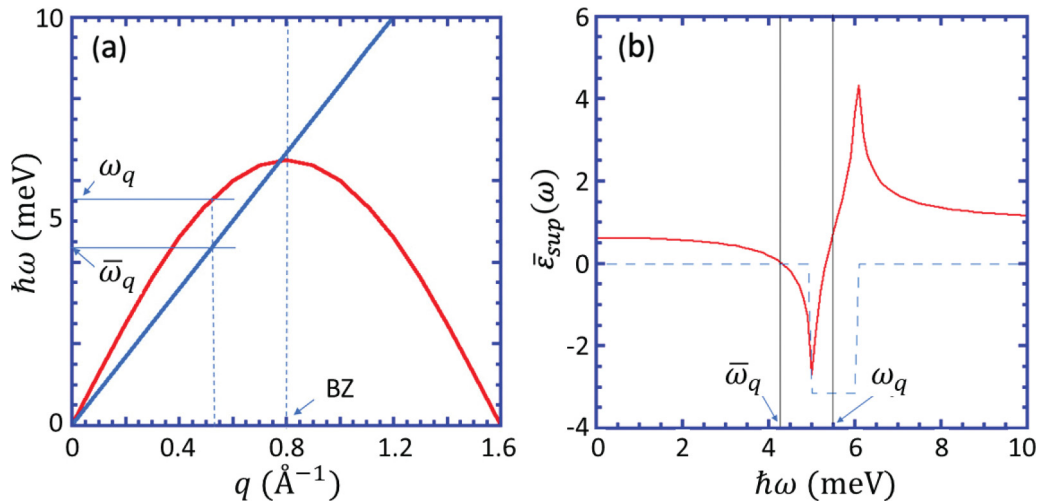
(2)

FIG. 2. (a) Collective modes of the 2D Dirac electron gas on the surface of a topological crystal Be_2Se_3 (interpolated from experimental data of Ref. [10]): $\alpha-$ mode (blue line), acoustic phonon mode (red line). BZ - Brillouin zone. (b) Calculated dielectric function of the 2D Dirac electron gas using Eq. (3) with a step model of $\alpha^2 F$, and assuming $\kappa = 1$. Solid line: real part, dashed line: imaginary part.

with dimensionless parameter (of order 1) $\kappa \sim k_F/\bar{\varepsilon}^2 > 0$, where k_F is the Fermi wave vector of the surface electrons in Bi_2Se_3, and the plasmon-polaron frequency is given by $\bar{\omega}_q^2 \approx \omega_q^2 - 2\kappa |g_q|^2 \omega_q$, and so $\bar{\omega}_q < \omega_q$. This frequency is confirmed by experiment [11] and theory [12]: the plasmon-polaron mode is negatively depolarization-shifted, i.e., it follows the phonon mode in the first BZ, but always at frequencies lower than the phonon mode [see Fig. 2(a)].

III. MODEL AND CALCULATIONS OF T_c

Consider now a superconductor film sandwiched between two TX slabs, as sketched in Fig. 1. We assume that the superconductor is sufficiently thin ($t_{sup} < 1/q \sim 1/k_F$), so that RAS is uniformly extended throughout the superconductor. The topological proximity effect, discussed below, can significantly relax this requirement [15]. Then, the effective dielectric function experienced by electrons in the superconductor is given by $\bar{\varepsilon}_{sup}(q, \omega) \approx \varepsilon_{sup} + [\varepsilon_{TI}(q, \omega) - 1]$, where ε_{sup} is ε of the bulk superconductor, of order 1 in the required domain of phase space, and the term in the square parentheses is the polarizability of the Dirac surface electrons of the topological Bi_2Se_3.

Phonons of the superconductor control the behavior of the plasmon-polaron, and we generalize Eq. (2) by relaxing the jellium assumption and by including all relevant phonon bands. Then, with $\epsilon_{\mathbf{k}}$ the electron energy, $g_{\mathbf{kk'}\nu}$ the generalized matrix element for scattering between electronic states $\mathbf{k}$ and $\mathbf{k'}$ through a phonon with $\mathbf{q} = (\mathbf{k'} - \mathbf{k}, \omega_{\mathbf{q}\nu})$ in phonon branch ν, and $\delta \to 0^+$, $\bar{\varepsilon}_{sup}$ becomes

$$\frac{\bar{\varepsilon}_{sup}(\omega)}{\varepsilon_{sup}} = \tilde{\varepsilon}_{sup}(\omega) = 1 - \kappa \left\{ \alpha^2 F(\omega) ln \left| \frac{\omega_{max} - \omega}{\omega_{min} - \omega} \right| \right.$$
$$+ \int_{\omega_{min}}^{\omega_{max}} \left[\frac{\alpha^2 F(\bar{\omega}) - \alpha^2 F(\omega)}{\bar{\omega} - \omega} + \frac{\alpha^2 F(\omega)}{\bar{\omega} + \omega} \right] d\bar{\omega}$$
$$\left. + i\pi \alpha^2 F(\omega) \right\}, \tag{3}$$

where we use the renormalized, dimensionless Eliashberg function $\alpha^2 F(\omega)$.

We can estimate the expected value of κ from experiment, by considering Bi_2Se_3 interfacing vacuum, in which case the phonon spectrum of Bi_2Se_3 controls the physics of the plasmon-polaron. Here, we model the Eliashberg function with a single dominant peak as a rectangle of height $\alpha^2 F(\omega) = 1$ in the range $\omega_{min} < \omega < \omega_{max}$, and $\alpha^2 F(\omega) = 0$ otherwise. Then, using Eq. (3), we obtain the result in Fig. 2(b) by assuming that $\kappa = 1$. This is in quantitative agreement with the experimental result shown in Fig. 2(a) at $q = 0.53 \text{Å}^{-1}$, which represents the maximum observed frequency difference, with $\Delta = \frac{\omega_q - \bar{\omega}_q}{\omega_q} \approx 20\%$. Since κ can be varied, we use it as an adjustable parameter in our present calculations. The Eliashberg function is screened, as is the generalized matrix element $|g_{\mathbf{kk'}\nu}|^2$, i.e., $\overline{\alpha^2 F(\omega)} = \alpha^2 F(\omega)/|\tilde{\varepsilon}_{sup}(\omega)|^2$. As mentioned, RAS occurs for $|\tilde{\varepsilon}_{sup}(\omega)| \ll 1$, and it strongly enhances the screened Eliashberg function. This is the main effect of RAS, and the next step is to calculate T_c from this screening-renormalized Eliashberg function. We first employ the *ab initio* solver

based on a direct solution of the coupled Eliashberg equations [16,17]. To calculate T_c, we solve directly the Eliashberg equations in Ref. [18]. The electron-phonon coupling function λ is computed from $\alpha^2 F$. Above the transition temperature, Δ vanishes. For the isotropic solver, we could choose to shield or to anti-shield $\alpha^2 F$. In principle, the same can be done for the anisotropic case. However, while only the anisotropic theory correctly predicts the observed two-gap superconductivity in MgB_2, it is also known to *overestimate* T_c in the absence of screening. Since the isotropic solver *underestimates* T_c by about the same fraction, we conservatively chose this solver for studying antishielding, and the fully anisotropic solver only to validate our code. Thus, our calculation with screening/RAS is expected to lead also to an underestimation of T_c, and consequently the ratio of T_c, with and without screening, is a rational way to quantify the superconductivity enhancement. Further details can be found in the Supplemental Material.

To support our *ab initio* calculations, we apply also the Leavens scaling method [19]. In contrast to many others (see [16]), this method is valid (as is *ab initio*) for arbitrary strength $\lambda = \int_0^\infty \frac{\alpha^2 F(\omega)}{\omega} d\omega$, required while dealing with RAS. The scaling method estimates not T_c, but its upper limit, i.e., $T_c^{max} = c(\mu^*) \int_0^\infty \alpha^2 F(\omega) d\omega$. The term $c(x)$ is a monotonically decreasing function of x (see Ref. [19]) and the Coulomb pseudopotential is

$$\mu^* \approx \frac{N(\mu)U}{1 + N(\mu)U \ln\left(\frac{\epsilon_F}{\hbar \bar{\omega}_q}\right)}, \tag{4}$$

where ϵ_F is the Fermi energy, and U is the double Fermi surface average of the screened Coulomb potential. Here, $\ln\left(\frac{\epsilon_F}{\hbar \bar{\omega}_q}\right)$ typically ranges from 5 to 10, and $N(\mu)U \gg \mu^*$. Thus, one can approximate Eq. (4) with $\overline{\mu^*} \approx \mu^* \approx \frac{1}{\ln\left(\frac{\epsilon_F}{\hbar \bar{\omega}_q}\right)}$, i.e., independent of $\tilde{\varepsilon}_{sup}(\omega)$. The general formula for T_c^{max} including antishielding, is given in this method by

$$T_c^{max} = c(\mu^*) \int_0^\infty \overline{\alpha^2 F(\omega)} d\omega = c(\mu^*) \int_0^\infty \frac{\alpha^2 F(\omega)}{|\tilde{\varepsilon}_{sup}(\omega)|^2} d\omega$$
$$= \frac{c(\mu^*)}{\kappa \pi} \int_0^\infty Im\left(\frac{1}{\tilde{\varepsilon}_{sup}(\omega)}\right) d\omega. \tag{5}$$

IV. APPLICATION TO MgB_2

We apply both calculational methods to MgB_2, the acknowledged highest T_c BCS-type superconductor (at ambient pressure), interfaced with Bi_2Se_3. We assume that phonons of MgB_2 control also the plasmon-polaron, and employ the *ab initio*-calculated $\alpha^2 F(\omega)$, with $\mu^* = 0.16$ [18,19]. Figure 3(a) shows the resulting T_c versus κ (red-solid circles), calculated by *ab initio* solving the Eliashberg equations, and assuming a uniform field of the plasmon-polaron Bi_2Se_3 inside MgB_2 (sufficiently thin film of MgB_2). For $\kappa = 0$ (absence of screening), the calculated T_c of 23 K is substantially lower than the experimental result of $T_c = 39$ K. The anisotropic calculation yields $T_c = 54$ K (open circle), i.e., substantially larger than experiment. T_c steadily increases with increasing κ, for $\kappa = 1.3$ has its maximum of ~ 100 K, and after that, rapidly decays. At the maximum, there is about
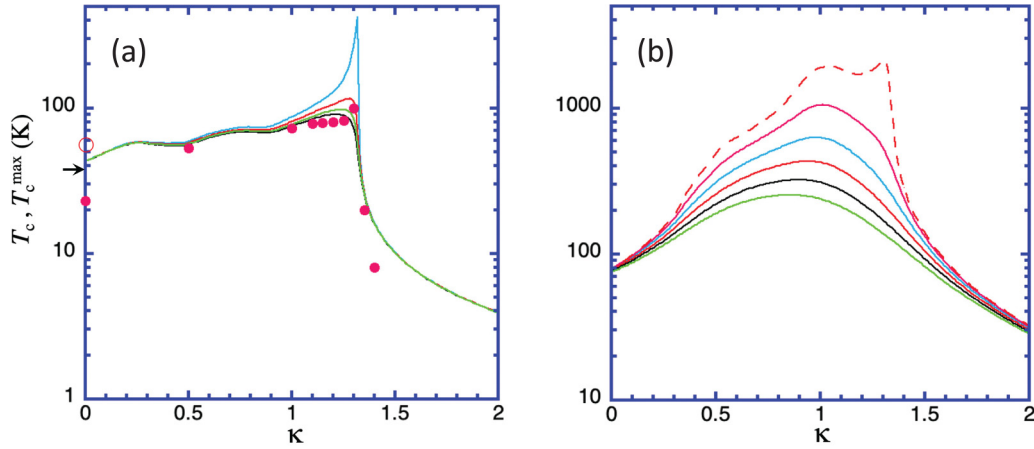
FIG. 3. (a) Calculated superconducting critical temperature T_c vs coupling parameter κ using the isotropic *ab initio* Eliashberg equations solution method for MgB_2, proximity coupled to Bi_2Se_3 (solid circles). Lines represent T_c^{max} vs κ obtained from the Leavens scaling method, for different quenching parameters ζ : 0 (blue line), 0.005 (red line), 0.008 (green line), and 0.01 (black-line). Open circle at $\kappa = 0$ is for the anisotropic case (see text). Arrow indicates experimental T_c. (b) T_c^{max} vs κ obtained from Leavens scaling for the YBCO- Bi_2Se_3 -MgB_2 structure, for different quenching parameters $\zeta = 0.01$ (dashed-red line), 0.05 (purple line), 0.1 (blue line), 0.15 (red line), 0.2 (black line), and 0.25 (green line).

fourfold enhancement of T_c, as compared to the case without screening ($\kappa = 0$).

Figure 3(a) shows also the T_c^{max} versus κ result (solid lines) obtained from Eq. (5), i.e., employing Leavens scaling. Surprisingly, $T_c^{max} = 43K$ at $\kappa = 0$, is much closer to the experimental result than the *ab initio* result, but the overall, qualitative shapes of all the scaling curves are the same. In fact, these curves are quite close to the *ab initio* result, with a significant departure only at the critical $\kappa = 1.3$ [see Fig. 3(a)]. This divergence results from the fact that at the RAS condition, $\tilde{\varepsilon}_{sup}(\omega)$ nearly vanishes, which can lead to a near singular behavior of the screened Eliashberg function. While the *ab initio* calculations seem unaffected by the problem, the scaling is affected. To remedy this, a small residual imaginary contribution $i\zeta$ (e.g., impurity scattering) can be added to $\tilde{\varepsilon}_{sup}(\omega)$, given by Eq. (3). The solid lines in Fig. 3(a) are calculated by varying ζ. Clearly, the main effect of this correction is to soften the divergence, and to drive the T_c^{max} curves closer to the *ab initio* result. The overall qualitative behavior of the curves in Fig. 3 can be understood analytically by using a toy model which employs $\varepsilon_{TI}(q, \omega)$ given by Eq. (2) as $\tilde{\varepsilon}_{sup}(\omega)$ in the very last part of Eq. (5). The resulting approximate formula is $T_c^{max} \sim [(\omega_q^2 - \kappa)^2 + \delta^4]^{-1/4}$. For $\kappa = 0$, it gives a finite result, at $\kappa = \omega_q^2$ it reaches a sharp maximum, and for $\kappa \to \infty$, it vanishes. These are the characteristics of all curves shown in Fig. 3.

Analysis of the above calculations indicates that further increasing of T_c by RAS is possible, if the superconductor phonon spectrum is not simultaneously controlling the Cooper pairing and the plasmon- polaron. This dominance of MgB_2 phonons forces (by the Kramers-Kronig relations) the near vanishing of $\tilde{\varepsilon}_{sup}(\omega)$ into the spectral domain of the nearly vanishing Eliashberg function. One intriguing possibility to avoid that would be to sandwich a TX (e.g., Bi_2Se_3) with a nonphonon mediated superconductor (e.g., YBCO) on one

side, and a phonon robust material (e.g., MgB_2) on the other. We consider such a case by: (a) using an experimentally-retrieved Eliashberg function for $YBa_2Cu_3O_{7-\delta}$ (YBCO) [20] with $c(\mu^*) = 0.2$; (b) by calculating the dielectric response from the *ab initio*-calculated Eliashberg function for MgB_2 [using Eq. (3)]; and (c) by applying Leavens scaling. Surprisingly again, for $\kappa = 0$, $T_c^{max} \approx 80$ K, close to the 92 K experimental value for YBCO, even though $c(\mu^*) = 0.17$ was chosen from the typical BCS range. As expected, the scaling method predicts diverging T_c^{max} at the critical point (again, near $\kappa = 1.3$), and to quench it, we use (as before) $i\zeta$. Figure 3(b) shows T_c^{max} *vs.* κ for this case, with each line calculated for a different ζ. The T_c^{max} divergence, clearly visible on the curve for $\zeta = 0.01$, is strongly damped for $\zeta = 0.05$, and completely disappears for $\zeta \geqslant 0.1$. By analogy to Fig. 3(a), one might expect the line for $\zeta = 0.1$ is not far from the T_c vs κ line and therefore [based on Fig. 3(b)], this structure might provide superconductivity at $T_c > 300$ K.

V. DISCUSSION AND CONCLUSION

The dimensionless coupling parameter κ can be controlled, e.g., through k_F (by adjusting the doping level in the plasmon-polaron host) and/or through $\bar{\varepsilon}$ (by changing the superlattice materials and/or dimensions). In addition, such T_c engineering might benefit from the topological proximity effect [15], at the surface of the TX $TlBiSe_3$ coated with superconducting Pb. It was shown that the topological state of the crystal extends up to 20 monolayers into the superconductor, without any admixing. This effect is expected to improve the plasmon-polaron penetration into the superconductor films of the superlattice, as well as could increase the efficiency of the phonon modifier layers.

Further possible architectures include natural or engineered bulk SC-TX layered materials, wherein the properties of the superconductor are modulated by the properties of

the proximate TX. For example, the cuprates consist of hole- or electron-doped CuO_2 layers sandwiched by non-conducting layers (e.g., yttrium- or bismuth- oxide). One could consider synthesizing cuprate systems modified to incorporate known TX layers (e.g., chalcogenides). Similarly, many organic superconductors are comprised of 2D superconducting layers sandwiched by nonconducting layers, the latter of which might be engineered to have TX character. The same *in situ* strategy could be applied to MgB_2, a BCS superconductor with very large, relevant phonon frequencies. Such incorporated topological modifications could produce atomic/molecular layers functioning as charge reservoirs as well as providing the T_c-enhancing RAS effect. These kinds of systems could facilitate high temperature superconductivity in multiple physical forms, from single crystalline to nanocrystalline / ceramic, so long as the core TX−superconductor−TX character was preserved.

In conclusion, we have demonstrated that a plasmon-polaron residing at the surface of a topological crystal interfaced with a superconductor can resonantly antishield Cooper pairs in the superconductor. This antishielding occurs regardless of the pairing mechanism, and leads to multifold enhancement of T_c.

[1] A. Schilling, M. Cantoni, J. D. Guo, and H. R. Ott, Superconductivity above 130 K in the Hg–Ba–Ca–Cu–O system, Nature (London) **363**, 56 (1993).

[2] V. L. Ginzburg and D. A. Kirzhnits, On the problem of high temperature superconductivity, Phys. Rep. **4**, 343 (1972).

[3] D. A. Kirzhnits, E. G. Maksimov, and D. I. Khomskii, The description of superconductivity in terms of dielectric response function, J. Low Temp. Phys. **10**, 79 (1973).

[4] V. L. Ginzburg, The problem of high-temperature superconductivity II, Sov. Phys. Usp. **13**, 335 (1970).

[5] I. I. Smolyaninov, and V. N. Smolyaninova, Theoretical modeling of critical temperature increase in metamaterial superconductors, Phys. Rev. B **93**, 184510 (2016); V. Smolyaninova, C. Jensen, W. Zimmerman, J. C. Prestigiacomo, M. S. Osofsky, H. Kim, N. Bassim, Z. Xing, M. M. Qazilbash, and I. I. Smolyaninov, Enhanced superconductivity in aluminum-based hyperbolic metamaterials, Sci. Rep. **6**, 34140 (2016).

[6] I. I. Smolyaninov and V. N. Smolyaninova, Metamaterial superconductors, Nanophotonics **7**, 795 (2018).

[7] D. R. Smith, J. B. Pendry, and M. C. K. Wiltshire, Metamaterials and negative refractive index, Science **305**, 788 (2004).

[8] R. D. Mattuck, *A Guide to Feynman Diagrams in the Many-Body Problem* (Dover, New York, 1976).

[9] A. J. Shvonski, J. Kong, and K. Kempa, Nonlocal extensions of the electromagnetic response of plasmonic and metamaterial structures, Phys. Rev. B **95**, 045149 (2017).

[10] X. Jia, S. Zhang, R. Sankar, F-C Chou, W. Wang, K. Kempa, E. W. Plummer, J. Zhang, X. Zhu, and J. Guo, Anomalous Acoustic Plasmon Mode from Topologically Protected States, Phys. Rev. Lett. **119**, 136805 (2017).

[11] A. Shvonski, J. Kong, and K. Kempa, Plasmon-polaron of the topological metallic surface states, Phys. Rev. B **99**, 125148 (2019).

[12] I. Bozovic, Low-energy collective electronic excitations in a polaron gas, Phys. Rev. B **48**, 876 (1993).

[13] G. Burns, *Solid State Physics*, (Academic, Orlando, 1985).

[14] R. Lyddane, R. Sachs, and E. Teller, On the polar vibrations of alkali halides, Phys. Rev. **59**, 673 (1941).

[15] C. X. Trang, N. Shimamura, K. Nakayama, S. Souma, K. Sugawara, I. Watanabe, K. Yamauchi, T. Oguchi, K. Segawa, T. Takahashi, Y. Ando, and T. Sato, Conversion of a conventional superconductor into a topological superconductor by topological proximity effect, Nat. Commun. **11**, 159 (2020).

[16] E. F. Marsiglio, and J. P. Carbotte, Electron-phonon superconductivity, in *Superconductivity*, edited by K. H. Bennemann and J. B. Ketterson (Springer, Berlin, 2008), pp. 73–162; F. Marsigilio, Eliashberg theory: A short review, Ann. Phys. **417**, 168102 (2020).

[17] G. M. Eliashberg, Interactions between electrons and lattice vibrations in a superconductor, Sov. Phys. JETP **11**, 696 (1960).

[18] E. R. Margine and F. Giustino, Anisotropic Migdal-Eliashberg theory using Wannier functions, Phys. Rev. B **87**, 024505 (2013).

[19] C. R. Leavens, A least upper bound on the superconducting transition temperature, Solid State Commun. **17**, 1499 (1975).

[20] E. G. Maksimov, M. L. Kulić, and O. V. Dolgov, Bosonic spectral function and the electron-phonon interaction in HTSC cuprates, Adv. Condens. Matter Phys. **2010**, 423725 (2010).